# Critical behavior of gelation probed by the dynamics of latex spheres

G. C. Fadda and D. Lairez*
*Laboratoire Léon Brillouin, CEA-CNRS, CEA/Saclay, 91191 Gif-sur-Yvette cedex, France*

J. Pelta
*ERRMECE, Université de Cergy-Pontoise, 95302 Cergy-Pontoise cedex, France*
(Received 21 November 2000; published 23 May 2001)

We report a quasielastic light scattering study of the dynamics of large latex probe particles ($R=225$ nm) in gelatin solution undergoing gelation. We show that by focusing on the short-time and long-time behavior of the autocorrelation function, it is possible to simply interpret out data in terms of the divergence of the viscosity and emergence of the shear elastic modulus near the gel point. Our crude analysis allows us to grasp the critical behavior of gelation and to obtain the two critical exponents of the transport properties.

DOI: 10.1103/PhysRevE.63.061405 PACS number(s): 82.70.Gg, 47.50.+d, 83.10.Pp

## I. INTRODUCTION

The use of spherical probe particles to study viscoelastic properties of polymer solutions has been suggested for a long time [1,2]. The basic idea is that in a semidilute solution of linear chains, sufficiently small particles freely move in the solution whereas larger particles would be trapped in the polymer transient network. Thus, the dynamics of probe particles is expected to be governed either by the solvent viscosity, or by the macroscopic viscosity, depending on their size $R$ compared to the correlation length $\xi_T$ of concentration fluctuations. A suitable technique to study such dynamics of probe particles is quasielastic light scattering, which has been extensively used on various physicochemical systems. According to the wide literature on this subject it appears that some complications may occur. For instance, a complex signal is sometime observed due to the contribution of the matrix and of the probe particles to the total light scattered intensity [3]. In addition, strong interactions between polymers in solution and particles, are sometimes reported which may cause adsorption of chains on the particles and particles aggregation [4,5]. However, it has been shown that, as soon as these complications are avoided, the basic idea is well founded. In particular for $R/\xi \gg 1$, the long-time dynamics of probe particles is slowed down and governed by the macroscopic viscosity [6–9] rather than the solvent viscosity.

Compared to rheology, the study of thermal fluctuations of concentration of probe particles for the investigation of weak structures is very attractive [10], because it guarantees the structure integrity. In particular, the use of probe particles for the study of gelation looks very tempting and has been already reported. Gelation [11] is a critical phenomenon of connectivity occurring when molecules randomly connect together leading at the gel point to a giant cluster: the gel. The understanding of quasielastic light scattering results obtained on gelling systems is much less clear as those obtained in semidilute solutions. On the one hand, gelation essentially produces a wide polydisperse population of clusters, which is responsible for complex relation processes. Therefore the analysis of the dynamical structure factor of probe particles in terms of time distribution is not quite obvious. On the other hand, above the gel point, fluctuations tend to be frozen at long-time because the solution becomes solid. This appears through a decrease in amplitude of the scattered intensity fluctuations. The most often used approach to account for this behavior invokes a loss of ergodicity [12–14]. The physical meaning of this approach consists in splitting the probe particles population into two parts: the first being free to diffuse in the medium, the second being trapped in the network and motionless. The scattered intensity has thus two contributions: a time fluctuating or quasielastic part and a constant or elastic part. Quasielastic light scattering technique consists in measuring the autocorrelation function of the scattered intensity. Consequently it also shows the two contributions. The first corresponds to the autocorrelation of the fluctuating part of the scattered intensity and the second to the correlation of this fluctuating part with the elastic scattering that acts as a local oscillator signal. In terms of the light scattering language, this amounts to mix a self-beating and a heterodyne contribution. Such an analysis calls for two remarks. First, the splitting of the probe particles population into two parts seems somewhat arbitrary and unsatisfactory. Second, above the gel point as fluctuations become more and more frozen the increasing heterodyne part leads at short time to a slowed dynamics while quite the opposite is experimentally observed [15].

In this paper, we present an analysis of quasielastic light scattering results from probe particles during gelation of a gelatin solution. We deliberately consider the simplest case, that is: (1) very large spherical and monodisperse latex particles (radius $R=225$ nm); (2) negligible thermodynamic interactions of probe particles between them or with the matrix; (3) a negligible contribution of the matrix to the scattered intensity; (4) measurements performed at $qR=1$ with $R/\xi_T \gg 1$. We show that, neglecting the nonergodicity and focusing on the short-time and long-time behaviors of the measured relaxation function, it is possible to simply interpret our data in terms of the divergence of the viscosity and emergence of a shear elastic modulus near the gel point. Our crude analysis allows us to grasp the critical behavior of gelation and to obtain the two critical exponents of the transport properties.

*Author to whom correspondence should be addressed.

 

## II. SAMPLE PREPARATION AND EXPERIMENTAL DEVICE

Gelatin was purchased from Sigma. Solutions of gelatin were prepared in 50 m*M* Tris-HCl buffer at $p\mathrm{H}=7.4$. Solubilization of gelatin was done at 40 °C. At this temperature, the intrinsic viscosity of gelatin was measured with a StressTech rheometer from Reologica. It was found to be $[\eta]=61\pm0.04\ \mathrm{cm}^3/\mathrm{g}$. The quasielastic light scattering experiments reported in this paper were performed at a gelatin concentration of 0.01 $\mathrm{g/cm}^3$.

Polystyrene latex particles were prepared and kindly provided by Loïc Auvray. The latex weight fraction of this initial preparation is $5.6\times10^{-2}$ g/g. It was determined by weighing after evaporation of water. This preparation was diluted by a factor of $3.25\times10^4$. Assuming a density of $\rho=1.05\ \mathrm{g/cm}^3$ for polystyrene this yields a final volume fraction of latex particles of $\phi=1.8\times10^{-6}$.

Light scattering measurements were performed with a home-made spectrometer using a krypton ion laser of wavelength $\lambda=647$ nm. Static light scattering measurements were performed for scattering angle $\theta$ between 10° and 150°, corresponding to scattering vector, $q=(4\pi n/\lambda)\times\sin(\theta/2)$, where $n=1.333$ is the refractive index of water, in the range $2.2\times10^{-3}-2.5\times10^{-2}\ \mathrm{nm}^{-1}$. Static measurements were done with toluene as reference (Rayleigh ratio equal to $8.5\times10^{-6}\ \mathrm{cm}^{-1}$). Toluene scattered intensity per unit scattering volume was found to be independent of the scattering angle within 1%. For static light scattering measurements on samples in the gel state, in order to obtain a correctly ensemble averaged intensity whatever the scattering angle, measurements were performed using a special device allowing the sample rotation during measurement. For this purpose, in order to minimize scattering due to optical defects, samples were contained in high optical quality cylindrical quartz cells (Hellma) having a large diameter of 25 mm. Quasielastic measurements were performed by computing the correlation function of the scattered intensity with a Malvern K7032 multitau correlator.

## III. STATIC LIGHT SCATTERING MEASUREMENTS

In Fig. 1 the ensemble and time averaged scattered intensity is plotted as a function of the scattering vector $q$. Measurements were performed on gelatin alone in the gel state, latex alone in solution, and latex plus gelatin solution at the same concentrations.

Let us first discuss the latex alone measurements (Fig. 1, hollow symbols). The $q$-dependent scattered intensity shows the classical oscillation of the form factor of a sphere: $S(q)=[3\{\sin(qR)-qR\times\cos(qR)\}/(qR)^3]^2$. Especially, the position of the first minimum or the periodicity of the oscillations, allow us to determine the radius of the latex particles as being $R=225\pm2$ nm. Note that these latex particles have a very narrow size distribution. This is particularly emphasized in the inset of Fig. 1, where $q^4I(q)$ is plotted as a function of $q$. In this representation, $q^4I(q)$ is close to zero at the first minimum corresponding to $q\equiv0.02\ \mathrm{nm}^{-1}$. This indicates a very good particle monodispersity. Knowing the shape of the

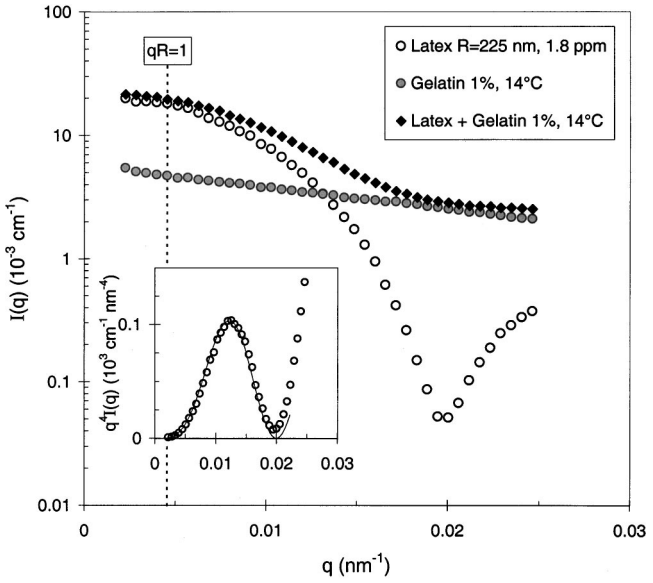


FIG. 1. Ensemble and time-averaged light scattered intensity per volume unit, $I(q)$, vs scattering vector $q$ measured for 1% gelatin alone solution in the gel state, latex alone solution (volume fraction $\phi=1.8\times10^{-6}$), and latex plus gelatin solution in the gel state at the same concentration. The dotted line corresponds to $qR=1$, with $R$ the radius of latex particles. In the inset, the classical representation $q^4I(q)$ vs $q$, outlines the very good monodispersity of latex particles (solid line corresponds to sphere form factor with $R=225$ nm).

form factor and the characteristic size of the particles, it is easy to extrapolate the scattered intensity to $q=0$. One gets $I(0)=(2.65\pm0.05)\times10^{-2}\ \mathrm{cm}^{-1}$. From the refractive index of polystyrene $n_{\mathrm{PS}}=1.595$, the contrast factor is calculated to be $K^2=[2\pi n(dn/dC)/\lambda^2]^2/N_A=4.56\times10^{-2}\ \mathrm{cm}^2\,\mathrm{g}^{-2}\,\mathrm{mol}$, where $N_A$ is Avogadro's number and $dn/dC$ the refractive index increment of polystyrene in water assumed to be equal to the difference $n_{\mathrm{PS}}-n$. Thus the forward scattered intensity gives a molar mass of latex particles: $M_{\mathrm{latex}}=I(0)/(\phi\rho K^2)=(3.00\pm0.06)\times10^{10}$ g/mol, which has to be compared to the calculated mass of one particle: $M_{\mathrm{calc}}=N_A\rho R^3 4\pi/3=3.02\times10^{10}$ g/mol. The very good agreement between these two values indicates that the latex volume fraction is so small that interactions can be neglected.

Measurements on the sample containing latex and gelatin (Fig. 1, black symbols) and comparison with the value measured for gelatin-alone solution (gray symbols) shows that the gelatin contribution may be neglected at small angles. In this $q$-range, the shape of the scattered intensity for latex plus gelatin sample is very close to the one obtained for latex alone indicating that no latex particles aggregation occurs.

In Fig. 2, the reciprocal scattered intensity per volume unit, $1/I(q)$, is plotted as a function of $q^2$, for the gelatin alone in the gel state. The scattered intensity can be fitted by an Ornstein-Zernike function: $I(q)=1/(1+q^2\xi_T^2)$, and gives the correlation length of concentration fluctuations, $\xi_T=43\pm4$ nm. This value is higher than the one already measured by small-angle neutron scattering for gelatin at this concentration [16]. This may be due to small heterogeneities that are commonly observed in gels [17]. However, it is notewor-

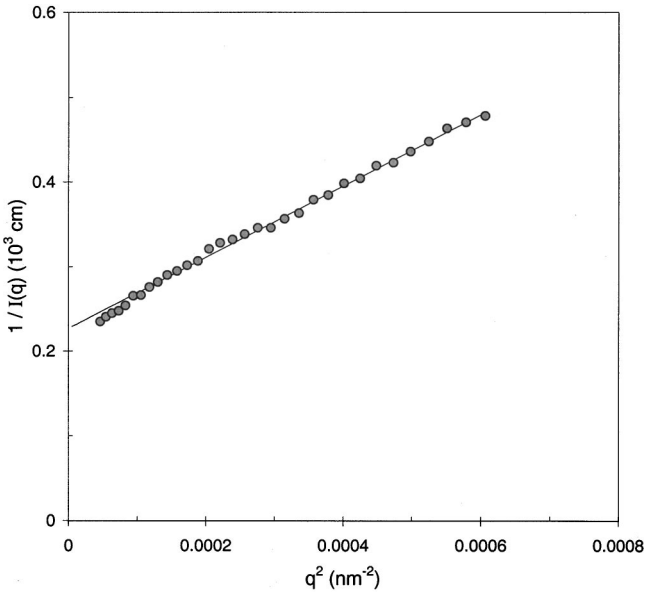


FIG. 2. Reciprocal scattered intensity per volume unit, $1/I(q)$, vs square scattering vector, $q^2$, for 1% gelatin alone solution in the gel state. The straight line corresponds to the best fit using an Orstein-Zernicke function for the scattered intensity: $I(q)=1/(1+q^2\xi_T^2)$, where $\xi_T=43\pm4$ nm is the correlation length of gelatin concentration fluctuations.

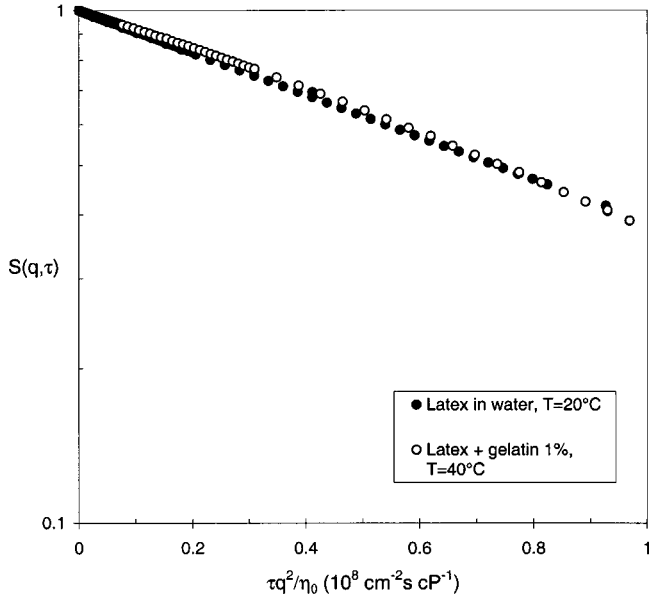


FIG. 3. Dynamical structure factor $S(q,\tau)$ for latex particles in water at 20 °C and for latex particles in 1% gelatin solution at 40 °C, vs $tq^2/\eta_0$, where $\eta_0$ is the viscosity of water ($\eta_0=1.002$ cP at $T=20$ °C and $\eta_0=0.653$ cP at $T=40$ °C).

thy that despite this higher value of $\xi_T$, the measured correlation length is much smaller than the latex particle size. Consequently, on the length scale of the latex particles, gelatin concentration is homogeneous.

## IV. QUASIELASTIC LIGHT SCATTERING MEASUREMENTS

Quasielastic measurements were done on latex solution in pure water at $T=20$ °C for scattering angles $\theta$ between 20° and 150°. The dynamical structure factor $S(q,\tau)$ has a simple exponential decay, with a characteristic time $\tau_c$ proportional to $q^{-2}$ as expected for diffusive motion. The corresponding diffusion coefficient is found to be $D_0=1/(\tau_c q^2)=(0.94\pm0.05)\times10^{-3}$ cm$^2$ s$^{-1}$. From the Stokes-Einstein relation, this value leads to the hydrodynamic radius $R_H=kT/(6\pi\eta_0 D_0)=228\pm12$ nm, where $kT$ is the thermal energy and $\eta_0$ the viscosity of water. This value is in very good agreement with the radius measured by static light scattering.

Measurements on latex particles were also performed in 1% gelatin solution at 40 °C in the liquid state. In Fig. 3, the dynamical structure factors $S(q,\tau)$, measured in pure water at 20 °C and in 1% gelatin solution at 40 °C, are plotted as a function $\tau q^2/\eta_0$, in order to account for trivial effect due to the temperature dependence of water viscosity. One can see that the initial decay rate of the structure factor remains unchanged with gelatin. Note that at 40 °C the viscosity of water is $\eta_0=0.653$ mPa s, whereas the macroscopic viscosity of the solution at the concentration $C=0.01$ g/cm$^3$, is $\eta=\eta_0(1+[\eta]C)=1.07$ mPa s. This proves that at this gelatin concentration and temperature, the solvent viscosity governs the short-time dynamics of latex particles. Moreover, this result shows that at 40 °C, no significant polymer adsorption occurs on the probe particles because such an adsorption would be revealed by an increase of the hydrodynamic radius of particles. In the following, we will show that the two above remarks are still valid at 17 °C, the temperature at which gelation was obtained.

In order to study gelation, the latex plus 1% gelatin solution, initially at $T=40$ °C, was quenched at 17 °C. Such a temperature ensures a gelation process sufficiently slow compared to the duration of one measurement. At $\theta=20°$, the autocorrelation of the scattered intensity was continuously measured during gelation by step of 10 min. In Fig. 4, the normalized autocorrelation function, $\langle I(0)I(\tau)\rangle/\langle I\rangle^2$, is plotted versus correlation time $\tau$, at different time $t$ during the gelation process (here brackets mean a time averaging). The shape of the autocorrelation function is no more a simple exponential decay. An accurate analysis of this shape is out of the range of this paper. However, in order to quantify the observed behavior, we have focused our analysis on the short-time and long-time behaviors. At short-time ($\tau<1$ ms), the autocorrelation function is characterized by the initial slope of the relaxation function: $(\langle I(0)I(\tau)\rangle/\langle I\rangle^2-1)^{1/2}\propto\exp[-(\tau/\tau_1)]$; whereas the long-time behavior was described by a stretched exponential: $(\langle I(0)I(\tau)\rangle/\langle I\rangle^2-1)^{1/2}\propto\exp[-(\tau/\tau_2)^\beta]$. Note that such a stretched exponential behavior for the long-time tail of the correlation function has already been reported and studied in details for gelling systems [18,19]. Although we did not check the short- and long-time dynamics behavior vary properly with $q$ (a multiphotodetector and a multichannel correlator are required for this), we will use the apparent diffusion coefficients, $D_S$ and $D_L$, defined as $D_S=1/(\tau_1 q^2)$ and $D_L=1/(\tau_2 q^2)$.

Without further data analysis, in Fig. 4 one distinguishes

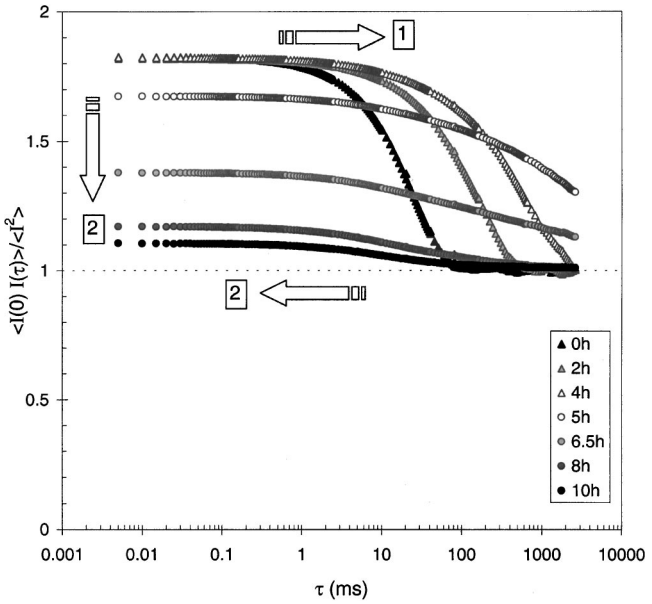


FIG. 4. Normalized autocorrelation function of the intensity scattered by latex probe particles, $\langle I(0)I(\tau)\rangle/\langle I\rangle^2$, vs correlation time $\tau$, for different time $t$ of the gelation process of 1% gelatin solution at $T=17\,^{\circ}\mathrm{C}$. Measurements were performed at a scattering angle $\theta=20\,^{\circ}$ corresponding to $qR=1$ for latex particles.

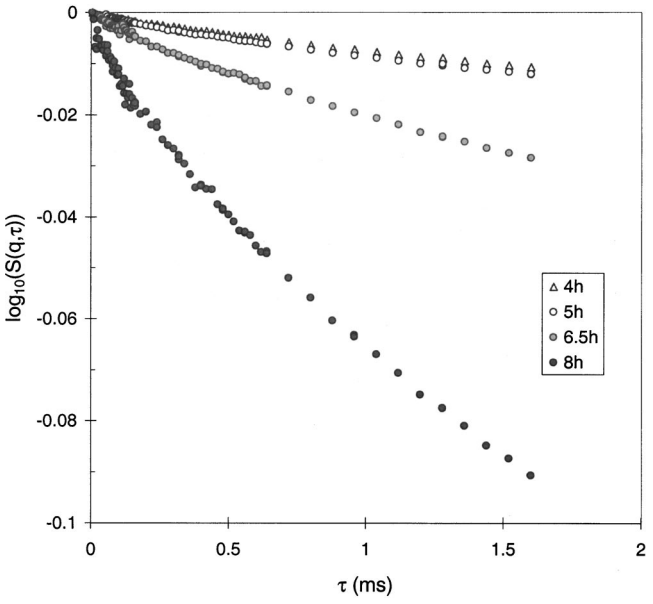


FIG. 5. Logarithm of the short time part of the dynamical structure factor $S(q,\tau)$ vs correlation time $\tau$, for different time $t$ of the gelation process (same experimental conditions as Fig. 4).

two stages during the gelation process:

(1) For gelation times $t$ shorter than 4.4 h the long-time tail of the normalized autocorrelation function shifts to even more long correlation times $\tau$ with a constant amplitude (triangles in Fig. 4,), whereas the short-time decay rate remains unchanged compared to the one observed in pure water.

(2) For gelation times $t$ higher than 4.4 h the amplitude of the normalized autocorrelation function drastically decreases, and the short-time behavior shifts to shorter correlation times (circles in Fig. 4). This short time behavior is much more emphasized plotting the logarithm of the dynamical structure factor as in Fig. 5. One can see that the initial decay rate increases as gelation goes on.

These two stages also appear clearly in Fig. 6, which shows that: before a gelation time $t_c$, the short-time dynamics is unaffected whereas the long-time dynamics slows down ($D_L$ tends toward 0 at $t_c$); beyond $t_c$, fluctuations decrease in amplitude and the short-time dynamics becomes faster ($D_S$ increases by a factor of 10).

As it will be discussed in the following section, the key point of our paper is that the change of the dynamics of probe particles in these two stages are linked to the critical behavior of gelation, namely, (1) divergence of the macroscopic viscosity below the gel point and (2) emergence of a shear elastic modulus above the gel point.

## V. DISCUSSION

### A. Short-time behavior in the liquid state

We observed at $T=40\,^{\circ}\mathrm{C}$ and in the liquid state at 17 °C, that the dynamics of the probe particles is governed at short-time by the solvent viscosity. Our quasielastic measurements were performed at a concentration $C$ corresponding to $[\eta]C=0.6$, i.e., just below the overlap concentration from the point of view of rheological properties. At this concentration, the data already reported in literature [16] as well as

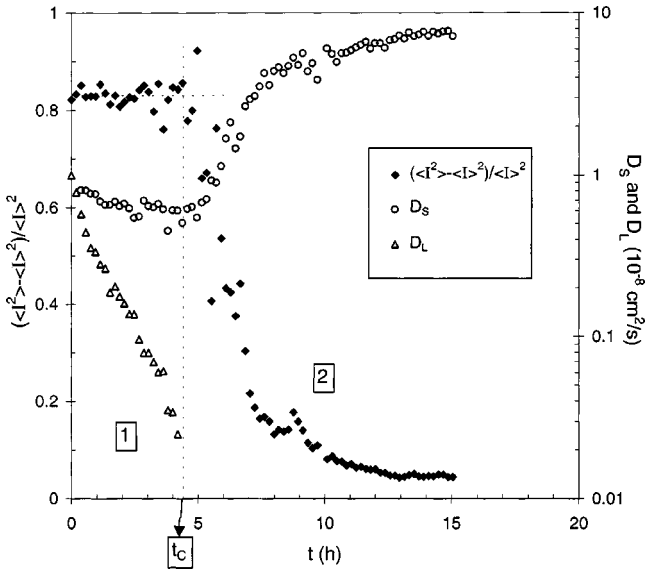


FIG. 6. Dynamics of latex probe particles during gelation of 1% gelatin solution at $T=17\,^{\circ}\mathrm{C}$. Full symbols: amplitude of the autocorrelation function of the intensity scattered by latex probe particles, $(\langle I(0)I(\tau)\rangle/\langle I\rangle^2-1)_{\tau\to 0}=(\langle I^2\rangle-\langle I\rangle^2)/\langle I\rangle^2$; Open triangles: long-time apparent diffusion coefficient $D_L$ deduced from a stretched exponential fit of the long-time tail of the correlation function; Open circles: short-time apparent diffusion coefficient $D_s$ deduced from the initial decay rate of the autocorrelation function. At $t_c=4.4\,\mathrm{h}$, $D_L$ tends to zero, fluctuations become frozen, and the short-time dynamics become faster.

our measurements (see Fig. 2) show that the correlation length of the concentration fluctuations $\xi_T$ is smaller than the size of the latex particles. In this situation, one would expect the matrix be viewed by latex particles as a continuum whose viscosity governs their dynamics. Therefore at first sight, a short-time dynamics governed by the solvent viscosity is puzzling. However, this behavior has been already observed for gelatin solutions [15] and, more generally, for polymer solutions near the overlap concentration [7]. In literature, it is often referred to as a ''positive deviation from Stokes-Einstein behavior.''

The first idea that would account for such a behavior is a diffusion mechanism within a cage [20] or in a harmonic potential [21]. Let us consider a latex particle in a semidilute solution (matrix) of correlation length $\xi_T$ and note $\langle r^2\rangle$ the mean-square displacement of the particle. The physical idea is that the polymer transient network does not affect the particle dynamics as long as $\langle r^2\rangle^{1/2}$ is smaller than $\xi_T$. Beyond $\xi_T$, if the particle size is larger than $\xi_T$, it begins to feel the transient network and to be slowed by the macroscopic viscosity. The dynamical structure factor of the particle can be written as $S(q,\tau)=\exp(-\langle r(\tau)^2\rangle q^2)$, with

$$\langle r(\tau)^2\rangle=\xi_T^2\left[1-\exp\left(-\frac{\tau}{\tau_S}\right)+\frac{\tau}{\tau_L}\right]. \tag{1}$$

Equation (1) comes from the expression used in the cage formalism [20,21]: the mean square displacement saturates to a plateau value $\langle r^2\rangle_{\text{plateau}}=\xi_T^2$ after a time $\tau_S$. Here, we have just added the term $\tau/\tau_L$, with $\tau_L$ larger than $\tau_S$, in order to account for the liquid state of the semidilute solution at long time. This point will be discussed in the following. Note that due to the nonzero viscosity inside the cage, the short-time dynamics is diffusive [10], $\langle r(\tau)^2\rangle\propto\tau$, rather than ballistic, $\langle r(\tau)^2\rangle\propto\tau^2$. A similar expression for $\langle r(\tau)^2\rangle$ has been used successfully for the description of the dynamics of telechelic triblock copolymers in semidilute solution [22]. In the latter case the transient cross-links of the network are dense copolymer micelles that give the major contribution to the light scattered intensity. Actually, the role of the osmotic modulus for the relaxation of concentration fluctuations can be viewed as being quite similar to the action of a spring constant $k_{\text{el}}$. Then, the characteristic time is $\tau_S=f/k_{\text{el}}$, where $f=6\pi\eta_0 R$ is the friction experienced by the particle and $k_{\text{el}}=kT/\xi_T^2$. One gets $\tau_S=\xi_T^2(6\pi\eta_0 R)/kT$, which leads to the short-time diffusion coefficient $D_S=\xi_T^2/\tau_S=kT/(6\pi\eta_0 R)$.

However, in our case the particle is larger than the cage and we propose in this paper a somewhat different mechanism. In general, the diffusion coefficient can be written as the ratio of an elastic energy to a friction. But for a given concentration fluctuation, what is the elastic energy and what is the friction? Let us consider the fluctuations of the particles and matrix concentration. At short-time, the driving force for relaxation of fluctuations is the matrix elastic modulus, i.e., in the liquid state the matrix osmotic modulus $K_{\text{matrix}}$. Then, the particles move in phase with the matrix and thus only experience the friction of the solvent. Therefore, we propose to write

$$D_S=\frac{\xi_T^3 K_{\text{matrix}}}{6\pi\eta_0 R}=\frac{kT}{6\pi\eta_0 R}. \tag{2}$$

Compared to the ''cage mechanism,'' the short-time diffusion coefficient is the same, but the characteristic time at which this mechanism begins to saturate is now shorter and corresponds to the relaxation time of the matrix osmotic modulus: $\tau_S=6\pi\eta_0\xi_T^3/kT$. At short time, the mean square displacement saturates at $\langle r^2\rangle_{\text{plateau}}=D_S\tau_S=\xi_T^3/R$, thus Eq. (1) may be rewritten as

$$\langle r(\tau)^2\rangle=\frac{\xi_T^3}{R}\left[1-\exp\left(-\frac{\tau}{\tau_S}\right)+\frac{\tau}{\tau_L}\right]. \tag{3}$$

The above ''matrix relaxation mechanism'' is faster than the ''cage mechanism'' and for this reason dominates the short-time behavior.

Very recently, Zanten and Rufener [9] have reported a study of brownian motion of latex particles in solution of entangled wormlike micelles. Their experimental results for the mean square displacement seems to be in very good agreement with our Eq. (3): short-time and long-time diffusive behaviors separated by a plateau region. This is a very nice textbook case because wormlike micelles are expected to display a pure exponential relaxation function at long-time [23]. The authors interpret their data in terms of diffusion in a Maxwell liquid, i.e., a liquid with a single relaxation time and a single viscosity. At short-time, the viscosity of a Maxwell liquid vanishes and the inertia of the particle cannot be neglected. Consequently, they expect a ballistic short-time behavior. However, the authors have experimentally shown that the short-time dynamics is slower and more compatible with that of a diffusion process. In our opinion, introducing the solvent local viscosity would solve this discrepancy. Except for this point, our approach is very similar to that of Zanten and Rufener. In particular Eq. (3) shows that the mean square displacement saturates at $\langle r^2\rangle_{\text{plateau}}=\xi_T^3/R=kT/(RK_{\text{matrix}})$, which is identical to the result obtained from the ''Maxwell liquid approach.''

### B. Long-time behavior in the liquid state

At times longer than $\tau_S$ the matrix has completely relaxed but not the particles, due to their longer characteristic time proportional to $R^3$ rather than $\xi_T^3$. Now, the remaining relaxation is thus only driven by the osmotic modulus of latex particles: $K_{\text{latex}}=nkT$, where $n$ is the number of particles per unit volume. In this time window, particles do not move in phase with the matrix and thus undergo the macroscopic viscosity $\eta$. The long-time diffusion coefficient $D_L$ is

$$D_L=\frac{K_{\text{latex}}/n}{6\pi\eta R}=\frac{kT}{6\pi\eta R}. \tag{4}$$

For polymer chains in solution, gelation occurs when chains are susceptible to link with each other and thus to form polymer clusters. Let us denote the number of links as $p$ and the size of the largest cluster as $\xi_C$. $\xi_C$ is the correlation length of connectivity, meaning that the probability for

two chains to belong to the same cluster is negligible for distances higher than $\xi_C$. Gelation is a critical phenomenon of connectivity: at the gelation threshold $p_c$ the correlation length $\xi_C$ tends toward infinity and so does the macroscopic viscosity as well [11]. As one approaches to the gelation threshold, it is expected that

$$\eta \propto \varepsilon^{-s}, \tag{5}$$

where $\varepsilon = |p - p_c|/p_c$ is the relative distance to the gelation threshold. Depending on the way hydrodynamic interactions are considered, different values are predicted for the exponent $s$. In presence of solvent (as opposed to bulk gelation), the most often reported [11] value is $s = 0.9 \pm 0.1$.

Gelatin is denatured collagen, a protein having a triple helix structure. Gelatin aggregation and gelation is due to the formation of helices between different polymer chains. It has been already shown [24] that the relevant quantity that accounts for the degree of connectivity is the helix amount $\chi$, which varies linearly with the logarithm of time whatever the concentration and the temperature. Thus, for the interpretation of our results, the appropriate expression for the relative distance to the threshold is

$$\varepsilon = \frac{|\chi - \chi_c|}{\chi_c} \tag{6}$$

with $\chi = a + b \times \ln(t) + \cdots$. For our purpose, which is to examine the gelation critical behavior, the exact expression for the time-dependent helix amount is not needed, but only its shape: $\chi \propto \ln(t)$ leading to $\varepsilon \propto \ln(t/t_c)$. However, in order to obtain quantitatively correct values for $\varepsilon$, the parameter $a$ and $b$ were estimated from Ref. [24]. In Fig. 7 (black symbols), the long-time diffusion coefficient $D_L$ is plotted as a function of the relative distance to the gelation threshold. As expected with respect to Eqs. (4) and (5), a power law behavior is found over more than one decade in $\varepsilon$:

$$D_L \propto \varepsilon^s \quad \text{with} \quad s = 0.85 \pm 0.10. \tag{7}$$

The value of the exponent $s$ is in very good agreement with the most often reported value deduced from rheological measurements.

Note that in order to account for the wide distribution of characteristic times, which is inherent to gelation and to the corresponding wide distribution of cluster sizes, the long-time tail of the correlation function is better described by a stretched exponential decay (see Sec. IV). Therefore Eq. (3) has to be replaced by an expression of the form: $\langle r^2 \rangle = (\xi_T^3/R)[1 - \exp(-\tau/\tau_S) + (\tau/\tau_L)^\beta]$. As the gelation threshold is approached, concomitantly with a decrease of $D_L$, we have observed a decrease of the exponent $\beta$ from 1 to 0.3. Such a behavior has already been reported for quasielastic experiments on gelling systems (without probe particles) [18,19].

### C. Short-time behavior in the gel state

At the gelation threshold, the appearance of a giant cluster is responsible for the emergence of a shear elastic modulus,

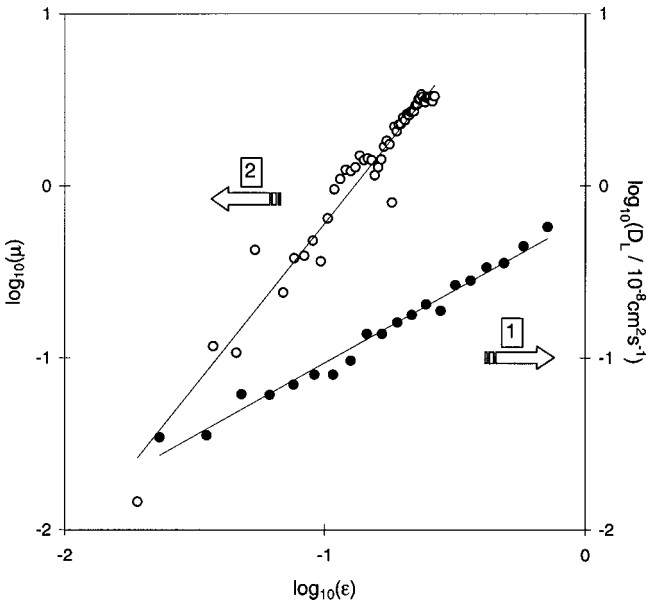


FIG. 7. Black symbols: logarithm of the long-time diffusion coefficient $D_L$ of latex particles before the gel point vs logarithm of the relative distance to the gelation threshold, $\varepsilon$. The straight line is the best linear fit. The corresponding slope is found to be $s = 0.85 \pm 0.1$. Hollow symbols: logarithm of the shear elastic modulus deduced from the amplitude of fluctuations, $\mu = [(\langle I^2 \rangle - \langle I \rangle^2)/b\langle I \rangle^2]^{-1/2} - 1$, measured after the gel point. The straight line is the best linear fit. The corresponding slope is found to be $t = 1.90 \pm 0.10$.

$G_{\text{matrix}}$. Actually, above the threshold this giant cluster is the gel phase that can be viewed as a polymer network of mesh size $\xi_C$. As for the macroscopic viscosity, gelation theories predict a power law behavior for the shear elastic modulus [11]

$$G_{\text{matrix}} \propto \varepsilon^t. \tag{8}$$

In the case of gelation in a solvent, the most often reported [11] value for the exponent $t$ is $t = 1.9 \pm 0.1$.

Light scattering experiments (as well as other scattering techniques) are sensitive to the longitudinal modulus $M$ of the sample that has a bulk (or compressibility) and a shear contribution. Neglecting density fluctuations and focusing only on concentration fluctuations, one can write [25]: $M = M_{\text{matrix}} = K_{\text{matrix}} + \frac{4}{3} G_{\text{matrix}}$. This longitudinal elastic modulus governs [26] the amplitude of the fluctuations. At $\tau = 0$ and $q = 0$, the dynamical structure factor $S(q, \tau)$ can be written as

$$S(0,0) = \frac{kT/\xi_T^3}{M_{\text{matrix}}}. \tag{9}$$

Since the short-time diffusion coefficient $D_S$ is almost constant before the gelation threshold (see Fig. 6), it appears that the osmotic modulus $K_{\text{matrix}}$ also does not significantly change [see Eq. (2)]. Let us assume that this is also the case above the gelation threshold. This is in agreement with the fact that gelation is a transition of connectivity ($\xi_C$ diverges

as $p$ tends toward $p_c$) and not a thermodynamic transition ($\xi_T$ is rather constant). Thus, $K_{\text{matrix}}=kT/\xi_T^3$ and Eq. (9) reduces to

$$S(0,0)=\frac{1}{1+\mu}$$

$$\text{with}\quad \mu=\frac{\frac{4}{3}G_{\text{matrix}}}{K_{\text{matrix}}}\propto G_{\text{matrix}}. \tag{10}$$

Let us neglect the possible problem due to nonergodicity (we will come back to this problem in the following). The autocorrelation of the scattered intensity is

$$\frac{\langle I(0)I(\tau)\rangle}{\langle I\rangle^2}=1+b[S(q,\tau)], \tag{11}$$

where $b$ is a constant lying between 0 and 1 and linked to the number of coherence areas viewed by the photodetector (in our experiments $b=0.8$). Assuming that Eq. (10) remains valid up to $qR=1$, one gets at $\tau=0$:

$$\left[\frac{\langle I^2\rangle-\langle I\rangle^2}{b\langle I\rangle^2}\right]^{1/2}=\frac{1}{1+\mu}. \tag{12}$$

Equation (12) means that the amplitude of fluctuations is constant in the liquid state ($\mu=0$) and decreases above the gelation threshold with the emergence of the shear elastic modulus. This is in agreement with our results. From the analysis of this decrease one can obtain the critical behavior of the modulus $G_{\text{matrix}}$. The ratio $\mu=G_{\text{matrix}}/K_{\text{matrix}}$ is deduced from Eq. [12] and from data shown in Fig. 6 (full symbols). In Fig. 7 (hollow symbols), $\mu$ is plotted as a function of the relative distance to the gelation threshold. As expected from Eq. (8), we observe a power law behavior over more than one decade in $\varepsilon$:

$$\mu\propto\varepsilon^t \quad \text{with} \quad t=1.90\pm0.10. \tag{13}$$

Here again, the value of the exponent $t$ is in very good agreement with the most often reported value deduced from rheological measurements.

According to our interpretation of the short-time behavior before the gelation threshold [see Eq. (2)], we would expect that above the threshold, the elastic modulus involved in the short-time dynamics is $M_{\text{matrix}}=K_{\text{matrix}}+\frac{4}{3}G_{\text{matrix}}$:

$$D_s=\frac{\xi_T^3\times M_{\text{matrix}}}{6\pi\eta_0 R}=\frac{kT}{6\pi\eta_0 R}\times(1+\mu)=D_0\times(1+\mu), \tag{14}$$

where $D_0=kT/(6\pi\eta_0 R)$ is the diffusion coefficient of latex particles in water at the same temperature. Therefore, above the gelation threshold, one expects a linear increase of the short-time diffusion coefficient $D_s$ as $\mu$ increases, i.e., as the amplitude of fluctuations decreases. This is actually observed (see Fig. 6). In Fig. 8, the ratio $D_s/D_0$ is plotted as a function of $\mu$. A linear behavior is found in agreement with Eq. (14). More specifically, extrapolation to $\mu=0$ (liquid state) leads to a diffusion coefficient $D_s=(0.95\pm0.10)\times D_0$, in good agreement with our expectation that at short time the friction encountered by the particles is only due to the solvent, in the liquid state as well as in the gel state. The slope in Fig. 8 is higher than the value predicted in Eq. (14). This point is not understood for the moment.

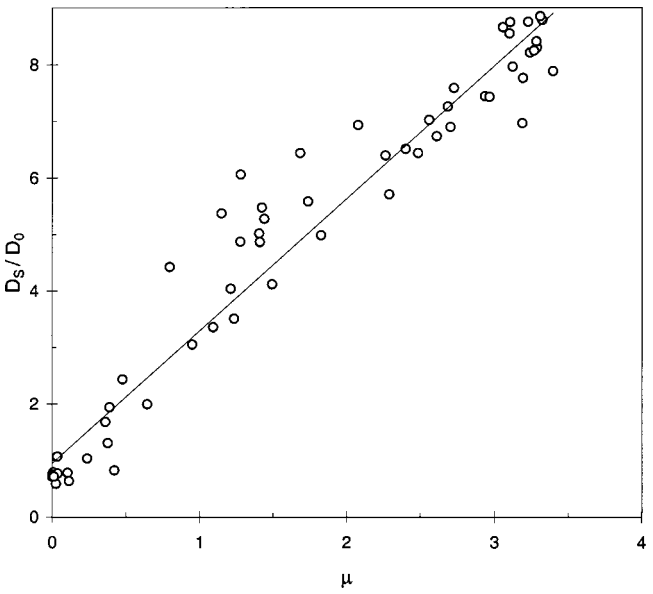


FIG. 8. Ratio of the short-time diffusion coefficient $D_s$ of latex particles measured during gelation to the diffusion coefficient $D_0$ expected in water at 17 °C vs $\mu=[(\langle I^2\rangle-\langle I\rangle^2)/b\langle I\rangle^2]^{-1/2}-1$. The straight line is the best linear fit corresponding to $D_s/D_0=0.95+2.34\mu$.

### D. Ergodicity or nonergodicity

Our interpretation for quasielastic light scattering on latex particles in gels is on the one hand very classical, because it comes directly from basic considerations on concentration fluctuations and longitudinal compressibility. On the other hand, this approach is different from the one commonly used for this problem. The main feature invoked for the interpretation of the dynamics in gels is the loss of ergodicity. Actually, in a gel, fluctuations are spatially frozen and the autocorrelation of the scattered intensity recorded by usual spectrometer is not an ensemble-averaged quantity. Different techniques are used to account for this problem and to extract the correct structure factor (time- and ensemble-averaged) from measurements [12,27]. As already mentioned, this approach consists in considering the scattered intensity as due to two contributions: a quasielastic part due to thermal fluctuations and an elastic part due to heterogeneities of the gel. Therefore, measurements mixes self-beating and heterodyne contributions [28]:

$$\frac{\langle I(0)I(\tau)\rangle}{\langle I\rangle^2}=1+b[y^2S(q,\tau)^2+2y(1-y)S(q,\tau)], \tag{15}$$

where $y=\langle I\rangle_E/\langle I\rangle_T$ is the ratio of the ensemble-averaged to the time-averaged intensity. In the case of probe particles in

a gel contribution of which to the scattered intensity can be neglected, the particle population is split into two parts [13]: a first part corresponds to the fraction $y$ of the total number of particles freely moving in the solution; a second part corresponds to the fraction $(1-y)$ of frozen particles. Let us focus on the short-time behavior predicted by this ''particle population splitting model.'' Denoting the initial decay rate of $S(q,\tau)$ as $\Gamma$, one has at short-time $S(q,\tau)=1-\Gamma\tau$ and $S(q,\tau)^2=1-2\Gamma\tau$. From Eq. (15), one gets

$$\frac{\langle I(0)I(\tau)\rangle-\langle I\rangle^2}{b\langle I\rangle^2}=y(2-y)-2y\Gamma\tau. \tag{16}$$

At $\tau=0$, the amplitude of the autocorrelation function decreases with decreasing fraction $y$ of moving particles. This latter expression has to be compared to our approach. Their physical meanings are completely different: Eq. (12) directly links the amplitude of fluctuations to the shear elastic modulus, whereas Eq. (16) involves an increasing fraction of frozen particles as the gel becomes stronger.

Within the ''particle population splitting model'' the apparent diffusion coefficient is $D_{\mathrm{app}}=\Gamma/[(2-y)q^2]$. This implies that at short time the dynamics is expected to be slowed down as the fluctuations become frozen. In the experiments reported here we have observed quite the opposite situation (see Fig. 6) and this suggests that experiments on gelatin solutions are not hindered by nonergodicity. Actually, this problem of ergodicity has to be considered with respect to the size of the scattering volume $V$ compared to the one of heterogeneities in the sample. Typically, $V$ is higher than $10^6\,\mu\mathrm{m}^3$. Such a volume can be considered as ''macroscopic'' with respect to the size of heterogeneity in gelatin gels. Therefore the distinction between ensemble-averaged and time-averaged scattered intensity is meaningless. Even though it could not be considered as ''macroscopic,'' problems would start as soon as the $q$ dependence of the autocorrelation function is considered, because the scattering volume depends on the scattering angle.

## VI. CONCLUSION

In this paper we have reported a quasielastic light scattering study of the dynamics of latex probe particles in a solution of gelatin undergoing gelation. We have shown that the long-time and short-time behaviors of the dynamical structure factor can be related to the macroscopic viscosity and to the elastic energy of the gelatin matrix, respectively. Before the gel point, the long-time tail of the dynamical structure factor shifts to even more long times as the macroscopic viscosity diverges. This result leads to the exponent for the dependence of the viscosity on the relative distance to the threshold: $s=0.85\pm0.1$. Above the gel point, the amplitude of fluctuations decreases drastically. We interpreted this behavior as being due to the emergence of a shear elastic modulus. Thus, the exponent for the dependence of the shear elastic modulus on the relative distance to the threshold was determined: $t=1.9\pm0.1$. To our knowledge, it is the first time that these two critical exponents for transport properties of gelling systems are obtained via quasielastic light scattering measurements. The values so determined are in very good agreement with those already obtained from rheological measurements on physical gels [11]. Moreover, our results are in good agreement with the earlier theoretical predictions based on the percolation model and on the electrical analogy [11] ($s=0.75$ and $t=1.9$). Very recently, more sophisticated theoretical approaches, allowing to study the different components of the stiffness tensor for percolating polymer networks, have been led to an exponent $t=1.95$, again in very good agreement with our result [29].

## ACKNOWLEDGMENTS

We thank L Auvray for providing us with the latex particles used for this work and P. Guenoun for viscosity measurements. We thank P. Calmettes for his attention to our first manuscript. Also, we would like to thank M. Djabourov for drawing our attention to the helix amount as the parameter for connectivity in gelatin solutions.

[1] P.-G. de Gennes, *Scaling Concept in Polymer Physics* (Cornell University Press, Ithaca, NY, 1979).
[2] D. Langevin and F. Rondelez, Polymer **19**, 875 (1978).
[3] See for instance the recent paper of: M. Shibayama, Y. Isaka, and Y. Shiwa, Macromolecules **32**, 7086 (1999).
[4] W. Brown and R. Rymdén, Macromolecules **19**, 2942 (1986); **20**, 2867 (1987).
[5] X. Ye, P. Tong, and L. J. Fetters, Macromolecules **31**, 5785 (1998).
[6] C. N. Onyenemezu, D. Gold, M. Roman, and W. G. Miller, Macromolecules **26**, 3833 (1993).
[7] J. Won, C. Onyenemezu, W. G. Miller, and T. P. Lodge, Macromolecules **27**, 7389 (1994).
[8] Z. Bu and P. S. Russo, Macromolecules **27**, 1187 (1994).
[9] J. H. van Zanten and K. P. Rufener, Phys. Rev. E **62**, 5389 (2000).
[10] T. G. Mason, H. Gang, D. A. Weitz, J. Mol. Struct. **383**, 81 (1996).
[11] See for instance a review paper: D. Adam and D. Lairez, in *The Physical Properties of Polymeric Gels*, edited by J.-P. Cohen-Adad (Wiley, New York, 1996), p. 87–142.
[12] J. G. H. Joosten, E. T. F. Geladé, and P. N. Pusey, Phys. Rev. A **42**, 2161 (1990).
[13] B. Carnins and P. S. Russo, Langmuir **10**, 4053 (1994).
[14] M. Kroon, G. H. Wegdam, and R. Sprik, Phys. Rev. E **54**, 6541 (1996).
[15] M. Djabourov, Y. Grillon, and J. Leblond, Polym. Gels Networks **3**, 407 (1995).
[16] I. Pezron, M. Djabourov, and J. Leblond, Polymer **32**, 3201 (1991).
[17] J. Bastide and S. J. Candau, in *The Physical Properties of Polymeric Gels*, edited by J.-P. Cohen-Adad (Wiley, New York, 1996), p. 143–308.
[18] J. E. Martin and J. P. Wilcoxon, Phys. Rev. Lett. **61**, 373 (1988).

[19] M. Adam, M. Delsanti, J.-P. Munch, and D. Durand, Phys. Rev. Lett. **61**, 706 (1988).
[20] F. Sciortino, P. Gallo, P. Tartaglia, and S.-H. Chen, Phys. Rev. E **54**, 6331 (1996).
[21] M. Doi and S. F. Edwards, in *The Theory of Polymer Dynamics* (Clarendon, Oxford, 1986).
[22] E. Raspaud, D. Lairez, M. Adam, and J.-P. Carton, Macromolecules **29**, 1269 (1996).
[23] M. E. Cates, J. Phys. (France) **49**, 1593 (1988).
[24] M. Djabourov, J. Leblond, and P. Papon, J. Phys. (France) **49**, 333 (1988).
[25] T. Tanaka, L. O. Hocker, and G. B. Benedek, J. Chem. Phys. **59**, 5151 (1973).
[26] Y. Rabin and A. Onuki, Macromolecules **27**, 870 (1994).
[27] J.-Z. Xue, D. J. Pine, S. T. Milner, X.-I. Wu, and P. M. Chaikin, Phys. Rev. A **46**, 6550 (1992).
[28] B. Chu, *Laser Light Scattering*, 2nd ed. (Academic, New York, 1991).
[29] O. Farago and Y. Kantor, Phys. Rev. Lett. **85**, 2533 (2000); Europhys. Lett. **4**, 413 (2000).